Fractionally Spaced Complex Sub-Nyquist Sampling for Multi-Gigabit 60 GHz Wireless Communication

Nicholas Preyss, Lorenz Koestler, and Andreas Burg
Telecommunications Circuits Laboratory, EPF Lausanne, 1015 Lausanne, Switzerland
e-mail: {nicholas.preyss, andreas.burg}@epfl.ch, lorenz@koestler.ch

***Abstract*—A novel analog front-end architecture based on complex sub-nyquist sampling for the intermediate frequency (IF) stage of a mmWave receiver is proposed. With this front-end, the use of a wideband hybrid coupler and two half-rate analog-to-digital converters (ADCs) allow for a flexible placement of the IF. It is shown that digital compensation of the impairments introduced by the non-ideal 90° hybrid coupler is required to use high modulation orders. Further a digital signal processing (DSP) architecture is presented which performs equalization of a fractionally spaced sub-sampled IF signal in frequency domain (FD) and integrates the compensation of the impairments with low overhead. Based on this DSP architecture a working 60 GHz single-carrier link is demonstrated. Measurement results show the feasibility of 256 QAM modulated transmission with a bandwidth of up to 1.8 GHz and a resulting raw data rate of 12.8 Gb/s using our frontend architecture with the digital FD compensation.**

I. Introduction

Limited available bandwidth and increasing interference levels due to over-utilization are currently the most dominant concerns for the further development of WiFi. Therefore, the large amount of available bandwidth as well as high spatial selectivity make the unlicensed spectrum at 60 GHz a promising candidate for future high throughput WiFi systems. For such 60 GHz systems the use of single carrier (SC) modulation regained popularity because of its low peak-to-average-power ratio (PAPR) which leads to relaxed requirements for the analog front-end compared to OFDM. In many 60 GHz use cases equalization of inter symbol interference is challenging due to the large delay spread. To combine the advantages of SC modulation with the excellent frequency equalization capabilities of OFDM the use of single carrier frequency domain equalization (SC-FDE) [1] is frequently proposed for wideband 60 GHz communication.

Many recently presented analog front-ends for 60 GHz systems are based on a heterodyne architecture [2][3]. As illustrated in Fig. 1a this radio architecture first downconverts the 60 GHz RF signal to an intermediate frequency (IF) passband signal for filtering. Afterwards the IF signal is down-converted by a second I/Q-demodulation stage to a complex baseband signal. The downside of the heterodyne architecture is the need for the additional hardware of the second conversion stage, which adds complexity to the system and potentially introduces new impairments.

As an alternative to analog down conversion from the IF, the concept of digital-IF gained popularity in recent years. In digital-IF receivers the complete IF signal is directly sampled and, down-conversion to baseband is performed afterwards in digital domain (cf. Fig. 1b). Such digital down-conversion requires that all information of the IF signal is retained during sampling. This can be achieved by extending the first Nyquist zone beyond the spectrum of the IF signal, at the expense of a potentially high sampling rate.

A third alternative is based on passband sub-sampling at the cost of additional constraints on the overall system design. These additional constraints render the use of passband sub-sampling problematic for software defined radio (SDR) receivers which require a large flexibility in the planning of frequencies and choice of bandwidth.

This work was partially supported by the Swiss National Science Foundation (NSF) project 200021_146753.

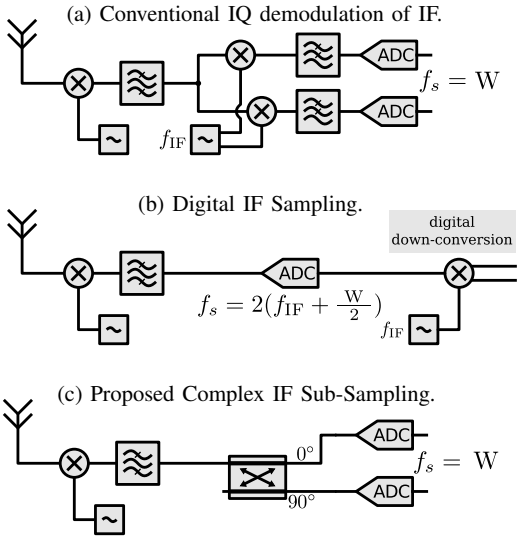

Fig. 1: Overview of different architectures for the IF stage of a wideband mmWave heterodyne receiver.

A. Contribution

In this paper a novel complex sub-nyquist sampling scheme for IF front-ends of Gigabit mmWave SDR is presented. The proposed scheme offers a high degree of freedom in the frequency planning due to a nearly arbitrary placable IF. Additionally a digital signal-processing architecture is proposed which not only compensates the impairments from the use of non-ideal hybrid coupler with low complexity, but offers also matched filtering, fractionally-spaced decimation and equalization. Using this signal-processing architecture the feasibility of QAM-256 modulation for mmWave communication is demonstrated with a 60 GHz link.

B. Outline

The paper is structured as follows. An introduction to the concept of sub-sampling and our proposed complex sub-sampling scheme is given in Section II. Afterwards, in Section III, we introduce the concept of frequency domain signal processing (DSP) and present a DSP architecture for complex sub-nyquist sampling based receivers. This is followed in Section IV by measurement results of a 60 GHz link using the proposed signal processing architecture. Finally in Section V we conclude the paper.

C. Notation

Throughout this paper we will denote time-domain signals with a lower case and frequency-domain signals with an upper-case designator. Further are continuous-time signals written with parentheses while discrete-time signals have brackets surrounding the time index. Hence the discrete-time samples $x[n]$ of the continuous-time signal $x(t)$ are found as $x[n] = x(n/f_s)$ with f_s being the sampling rate.

We further denote the 2π-periodic expansion of a $\pi < \omega \leq \pi$ band-limited signal $X(\omega)$ with a tilde as $\tilde{X}(e^{j\omega}) = \sum_{i=-\infty}^{\infty} X(\omega - 2\pi i)$.

II. Complex Sub-Nyquist Sampling

Sub-nyquist sampling is a well known technique to reconstruct a passband signal with components above half the sampling rate f_s, if there is additional knowledge about the structure of the signal. In particular it is necessary that the bandwidth W of the signal does not exceed $\frac{f_s}{2}$ and it must completely reside within a Nyquist zone [4]. These conditions can be easily seen from the frequency-domain description of the sampling operation. The discrete time fourier transform (DTFT) spectrum $\hat{X}(e^{j\omega})$ of a signal $x[n]$, sampled at rate $f_s = \frac{1}{T_s}$, is given as

$$\hat{X}(e^{j\omega}) = \frac{1}{T_s} \sum_{k=-\infty}^{\infty} X\left(j\frac{\omega}{T_s} - j\frac{2\pi k}{T_s}\right), \tag{1}$$

where $X(\omega)$ is the Fourier transform of the continuous-time signal $x(t)$ [5]. Hence the spectrum $\hat{X}(e^{j\omega})$ of the sampled signal is a 2π-periodic folding of shifted copies of $X(\omega)$. Consequently if the desired signal is confined in a Nyquist zone as shown in Fig. 2a the aliases due to sub-sampling do not overlap (cf. Fig. 2b). The original signal can still be reconstructed after sampling at the Nyquist rate $f_s = 2\mathrm{W}$.

If the IF signal crosses the boundary of a Nyquist zone (cf. Fig. 2c), corruption of the signal occurs due to the negative and positive frequency components folding on top of each other (cf. Fig. 2d). In narrow band systems this problem is usually mitigated by applying over-sampling and thereby increasing the size of the Nyquist zones until it encompasses the desired IF band completely.

Unfortunately for mmWave systems with signal bandwidth significantly above 1 GHz the sampling rate can not be easily increased. Therefor the list of candidate frequencies for the IF is restricted to a set of very few points and hence complicates significantly frequency planning and the usefulness of sub-sampling architectures.

A. Ideal case

In order to lift this restriction, we propose a complex sub-nyquist sampling strategy, which allows a flexible placment of the IF. Complex sub-sampling has been proposed in [6] for 60 GHz using phase-shifted sampling clocks. In our system a complex-valued analytic representation of the IF signal in analog domain is generated by means of a wide-band 90° hybrid coupler. A 90° hybrid coupler splits the signal energy of an input $x(t)$ and outputs it on two ports $x_I(t)$ and $x_Q(t)$ with a 90° phase offset in between. Such a 90° phase shift corresponds to a Hilbert transformation $\mathcal{H}\{\cdot\}$ of a signal, which is given in frequency-domain by[1]

$$\mathcal{H}\{X(\omega)\} = \begin{cases} -jX(\omega) & ,\omega \geq 0 \\ +jX(\omega) & ,\omega < 0. \end{cases} \tag{2}$$

The two analog output signals are synchronously sampled and represent the real and imaginary part of an analytic version of the IF signal

$$\bar{X}(\omega) = X_I(\omega) + j\mathcal{H}\left(X_I(\omega)\right). \tag{3}$$

The resulting analytic signal $\bar{X}$ is characterized by that it has no negative frequency components.

As illustrated in Fig. 2f, no corruption will occur independently of the position of the IF signal during sub-sampling of an analytic signal. Note that the analytic signal is now complex-valued, therefor two analog to digital converters (ADCs) at a sampling rate of $f_s = W$ are required. Nevertheless the resulting complex sub-sampled signal can still be rotated by a ω_{off} offset in frequency domain as shown in Fig. 2f. Fortunately due to the 2π-periodicity of the spectrum a multiplication with $e^{-j\omega_{\mathrm{off}}t}$ rotates the signal at the correct place in the spectrum.

[1] As we apply the Hilbert transformation to passband signals only we will accept for compactness a certain imprecision about the case $\omega = 0$.

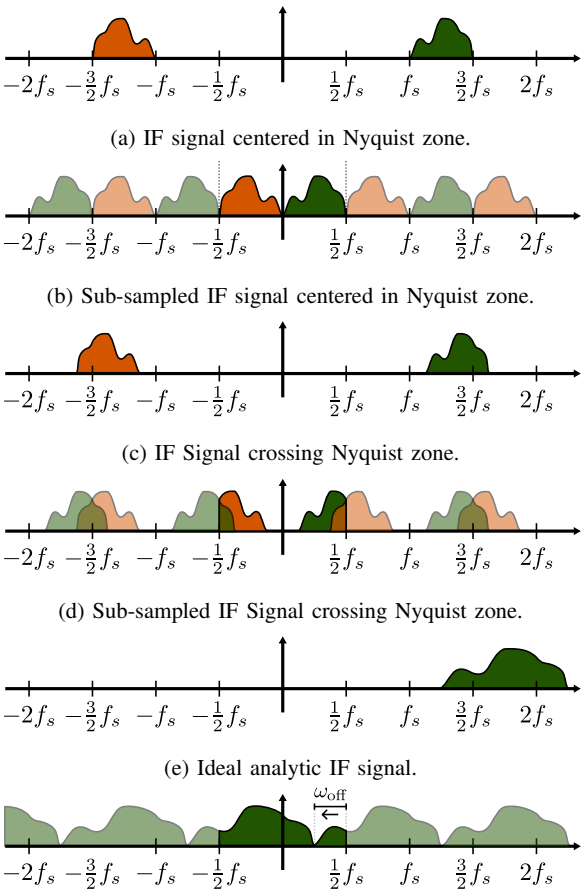

(a) IF signal centered in Nyquist zone.

(b) Sub-sampled IF signal centered in Nyquist zone.

(c) IF Signal crossing Nyquist zone.

(d) Sub-sampled IF Signal crossing Nyquist zone.

(e) Ideal analytic IF signal.

(f) Sub-sampled ideal analytic IF signal.

Fig. 2: The effect of Nyquist rate sub-sampling on the spectrum of an IF signal. The positive frequency component is marked with green, the negative frequency component with orange color.

B. Non ideal case

A downside of the use of a hybrid coupler is the introduction of a significant amount of port-specific frequency selectivity over the bandwidth of interest. This can lead to a potential mismatch between the two sampling paths. As a result the imperfection of the hybrid coupler poses the biggest challenge for the integration of complex sub-nyquist sampling in mmWave receivers. A deviation from the ideal 90° phase offset and a mismatch in the magnitude response of the two output branches lead to an incomplete suppression of the negative frequency component. To capture this effect, we introduce $H_I(\omega)$ and $H_Q(\omega)$ to describe the frequency selectivity of the two output branches of the coupler and their baseband equivalents

$$G_I(\omega) = \begin{cases} H_I(\omega + \omega_{\mathrm{IF}}) & ,\pi < \omega \leq \pi \\ 0 & ,else \end{cases} \tag{4}$$

and

$$G_Q(\omega) = \begin{cases} H_Q(\omega + \omega_{\mathrm{IF}}) & ,\pi < \omega \leq \pi \\ 0 & ,else. \end{cases} \tag{5}$$

Further we note that now the real-valued passband IF signal $X(\omega) = X_I(\omega) + jX_Q(\omega)$ can be expressed as function of the complex-valued baseband signal $B(\omega)$. Consequently we find

$$X_I(\omega) = H_I(\omega)B(\omega - \omega_{\mathrm{IF}}) + H_I^*(-\omega)B^*(-(\omega + \omega_{\mathrm{IF}}))$$

and

$$X_Q(\omega) = -jH_Q(\omega)B(\omega - \omega_{\mathrm{IF}}) + jH_Q^*(-\omega)B^*(-(\omega + \omega_{\mathrm{IF}})).$$

After sub-sampling and a shift by ω_{off}, the two resulting signals

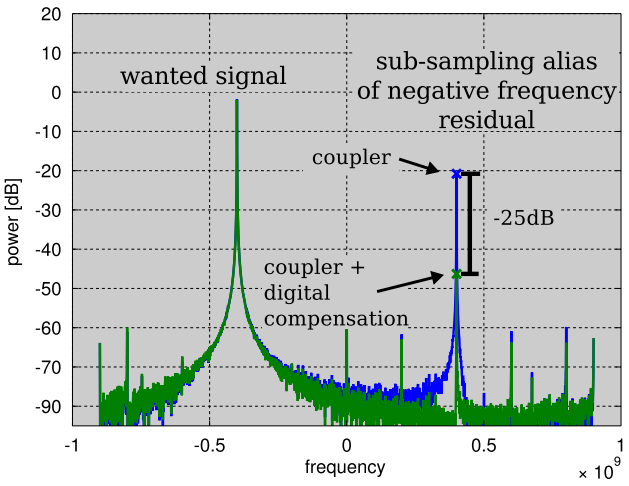

Fig. 3: Surpression of the negative frequency components of a narrow band test signal after complex-subsampling.

are given by

$$X_I(e^{j\omega}) = \tilde{G}_I(e^{j\omega})\tilde{B}(e^{j\omega}) + \tilde{G}_I^*(e^{-j\hat{\omega}})\tilde{B}^*(e^{-j\hat{\omega}}) \quad (6)$$

and

$$X_Q(e^{j\omega}) = -j\tilde{G}_Q(e^{j\omega})\tilde{B}(e^{j\omega}) + j\tilde{G}_Q^*(e^{-j\hat{\omega}})\tilde{B}^*(e^{-j\hat{\omega}}), \quad (7)$$

where $\hat{\omega} = \omega + 2\omega_{\text{off}}$. Applying now $X(e^{j\omega}) = X_I(e^{j\omega}) + jX_Q(e^{j\omega})$ leads to the desired signal

$$X_s(e^{j\omega}) = (\tilde{G}_I(e^{j\omega}) + \tilde{G}_Q(e^{j\omega}))\tilde{B}(e^{j\omega}) \quad (8)$$

and a residual error term

$$X_e(e^{j\omega}) = (\tilde{G}_I^*(e^{-j\hat{\omega}}) - \tilde{G}_Q^*(e^{-j\hat{\omega}}))\tilde{B}^*(e^{-j\hat{\omega}}) \quad (9)$$

which is only zero when $\tilde{G}_I(e^{j\omega}) = \tilde{G}_Q(e^{j\omega})$. Therefore, when the signal is sub-sampled, corruption due to aliasing will occur. The resulting error term can not be corrected with the channel equalizer of the system which treats the signal as a complex-valued signal. Instead independent equalization of the real and the imaginary part of the IF signal is required in order to compensate the frequency-dependent mismatch and obtain a good suppression of the negative frequency components. The compensation has to take the effect of the aliasing into account, hence the equalizer coefficients E can be found as $\tilde{E}_I(e^{-j\omega}) = (\tilde{G}_I^*(e^{-j\hat{\omega}}))^{-1}$ and $\tilde{E}_Q(e^{-j\omega}) = (\tilde{G}_Q^*(e^{-j\hat{\omega}}))^{-1}$. After equalization the folded negative components of real and imaginary part perfectly cancel each other.

Using a narrow-band signal, we can assure that during the complex sub-sampling the positive and the partly suppressed negative frequency components do not fold onto each other. This special case can be used to directly measure the aliasing with and without our compensation of the branch mismatch. In Fig. 3 we can see that even without compensation already a significant suppression of the negative frequency component is achieved by the hybrid coupler. Applying the proposed equalization reduces the power level of the residual component by another 25 dB. Note that these measurements of a very narrow-band signal have been performed after directly connecting the IF source to the hybrid coupler without a 60 GHz channel in between.

III. Digital Signal Processing Architecture

For our DSP architecture we assume the frame format of the SC physical interface in the IEEE802.11ad standard [7] as illustrated in Fig. 4. A short training field (STF) for synchronization at the beginning of each frame is followed by a channel estimation field (CEF) containing two 512 symbol long complimentary Golay sequences and a 128 symbol periodic extension for termination. The following data field is segmented in blocks of 512 symbols, of which the first 448 symbols carry information, while the last 64 symbols

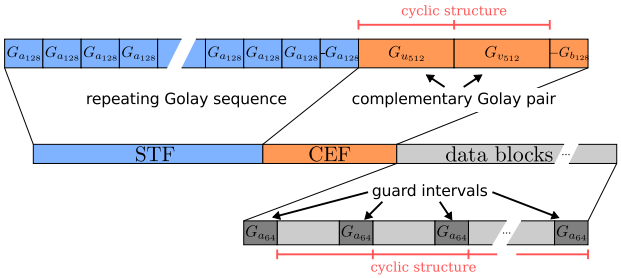

Fig. 4: Frame format as specified in the IEEE802.11ad standard for 60 GHz communication. The CEF and the data blocks exhibit a cyclic structure with a block length of 512 symbols.

serve as a known guard interval (GI) sequence. The chosen frame structure assures that not only the data but also the CEF exhibits a cyclic property with a block length $N_{\text{BLK}} = 512$.

A. Frequency-domain equalization

First we give a short introduction how the cyclic structure can be used to perform most of the baseband signal processing computationally efficient in frequency domain. Afterwards we show how such an architecture can be adapted with very little additional complexity to integrate the signal processing that is specific to our complex sub-sampling.

The basic frequency-domain signal processing chain is shown in Fig. 5. Over-sampling is applied in order to capture the full bandwidth of the pulse-shaped signal and enable the use of a digital matched filter for precise noise filtering and timing offset correction. As outlined before increasing the sampling rate is costly in extreme wide-band systems, therefor we try to design the system with the least amount of oversampling required. The corresponding oversampling factor N_{OS} is chosen close to $1 + r_{\text{RRC}}$ in order to match the excess bandwidth of the pulse shape, where r_{RRC} being the rolloff factor of the used root-raised cosine (RRC) pulse. This choice results in fractionally-spaced sampling with a system bandwidth of $\text{W} = f_{\text{sym}} N_{\text{OS}}$.

The fractionally-spaced samples are converted to frequency-domain by using a fast Fourier transform (FFT) with a block size of $N_{\text{FS}} = N_{\text{BLK}} \cdot N_{\text{OS}}$ to match the cyclic structure of the frame. The N_{FS} resulting fractionally-spaced samples are then filtered in frequency-domain with the spectrum of the RRC pulse.

After matched filtering, the frequency-domain signal is first decimated to symbol rate by cyclic folding of the excess bandwidth (cf. Fig. 5) and subsequently equalized to compensate the frequency-selectivity of the channel. Decimation before equalization allows the channel estimation to be performed with an symbol spaced time-domain channel estimator [8]. Afterwards the equalized frequency-domain samples are converted back to time-domain by using the inverse FFT (IFFT) with block length N_{BLK} and forwarded to the channel estimator or a slicer.

B. Frequency-domain hybrid coupler compensation

The basic FDE architecture shown in Fig. 5 can be extended to perform the signal-processing required for our proposed complex

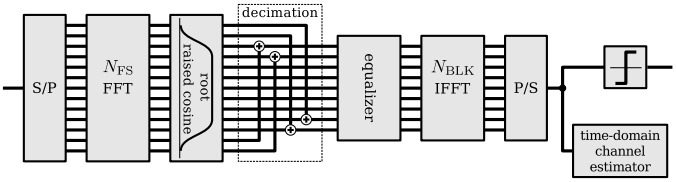

Fig. 5: Frequency domain architecture for matched filtering, decimation and equalization.

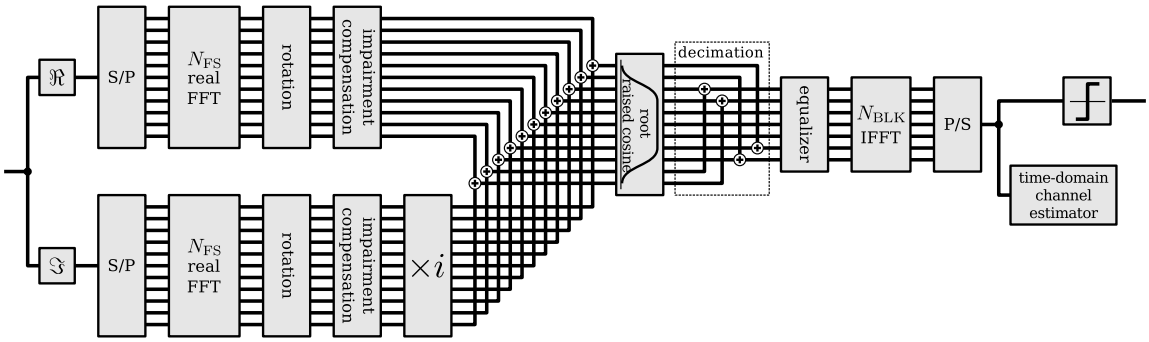

Fig. 6: Overview of the proposed frequency-domain digital signal processing architecture for a complex sub-sampling receiver.

TABLE I: 60 GHz Link Setup

carrier frequency	61 GHz
intermediate frequency	1.8 GHz
symbol rate	1.6 GS/s
sampling rate	1.8 GHz
pulse shape	RRC
roll-off factor	0.12
modulation	256-QAM
raw data rate	12.8 Gb/s
FFT / IFFT block size	576 / 512

sub-sampling receiver. By using the fact that the cyclic structure of the frame applies also to the real and imaginary parts of the signal, the FFT can be applied to both dimensions separately (cf. Fig. 6). Fortunately this split of the FFT comes without a significant increase in system complexity as a complex-valued FFT can be used to compute the FFT of two real valued sequences simultaneously [9]. A residual frequency shift ω_{off} can now be compensated by simple rotation of the frequency indices of the samples. Both branches can now be equalized separately using the respective frequency response of the coupler as described in Section II and recombined afterwards to the frequency-domain baseband signal. The resulting signal can be further processed as outlined in the previous section.

IV. 60GHz Link Measurement

In order to demonstrate the potential of the proposed DSP architecture, a 60 GHz short range link was setup. A high-quality signal for the transmitter was generated by means of a Tektronix AWG7122C arbitrary waveform generator. In the transmitter and the receiver a pair of commercially available Sivers IMA FC1005V 60 GHz front-ends are used for conversion between the IF signal and the 60 GHz band. Transmission was performed over a distance of approximately 0.2 m. At the receiver the complex IF signal for sampling is generated with a MECA 705S-3.000 3dB 90° hybrid coupler. Sub-nyquist sampling of the IF signal was performed using a TI ADC12D1800RF dual ADC with a sampling rate of up to 1.8 GS/s and an analog bandwidth of up to 2.7 GHz. The IF signal is placed at an intermediate frequency of 1.8 GHz to still reside within the analog bandwidth of the ADCs. The ADC streams the sampled data to an FPGA via a high-speed LVDS interface.

The transmitted signal is single-carrier modulated using 256-QAM and a symbol-rate of 1.6 GS/s, which results in a raw data rate of 12.8 Gb/s. A detailed list of the link parameters can be found in Table I. Due to the used IEEE802.11ad compliant frame format 11.2 Gb/s are usable for information bits because of the periodic GI. At the receiver the data was sampled with a fractional over-sampling factor of $N_{\mathrm{OS}} = 1.125$. The constellation diagram of the received symbols without coupler compensation is shown in Fig. 7a, applying the compensation leads to the clear constellation diagram shown in Fig. 7b. With compensation enabled a BER of below 0.5% can be achieved. This demonstrates the potential of our propsed DSP architecture for high order modulation 60 GHz links.

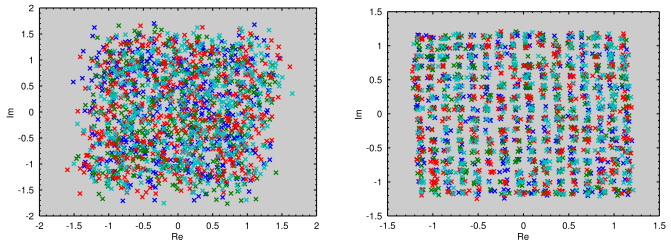

(a) without compensation (b) with compensation

Fig. 7: Received 256-QAM symbols transmitted over a 60 GHz link with a data rate of 12.5 GBit/s using the proposed DSP architecture.

V. Conclusion

We have presented a novel complex sub-sampling IF architecture for wide-band mmWave SDR receivers using 90° hybrid couplers to generate an analytic representation of the IF signal. The impairments introduced by the non-ideal couplers can be effectively compensated by separate equalization of the real components of the analytic IF signal. A proposed digital signal processing architecture exploits the cyclic structure of the IEEE802.11ad frame format to combine impairment compensation with channel equalization in frequency domain. Measurements show that the high achievable linearity enables high order modulation. The effectivness of the proposed equalization architecture could be demonstrated with a 256-QAM modulated 60 GHz link with a data rate of up to 12.8 Gb/s.

References

[1] D. Falconer, S. L. Ariyavisitakul, A. Benyamin-Seeyar, and B. Eidson, "Frequency domain equalization for single-carrier broadband wireless systems," *IEEE Commun. Mag.*, vol. 40, no. 4, pp. 58–66, 2002.

[2] C.-S. Choi *et al.*, "60-Ghz OFDM systems for multi-gigabit wireless LAN applications," in *Consumer Communications and Networking Conference (CCNC), 2010 7th IEEE*, 2010, pp. 1–5.

[3] F. Barale *et al.*, "Pulse shaping and clock data recovery for multi-gigabit standard compliant 60 GHz digital radio," in *Microwave Symposium Digest (MTT), 2010 IEEE MTT-S International*, 2010, pp. 908–911.

[4] W. Kester, "What the nyquist criterion means to your sampled data system design," *Analog Devices*, pp. 1–12, 2009.

[5] P. Prandoni and M. Vetterli, *Signal processing for communications*. CRC Press, 2008.

[6] B. Grave, A. Frappe, and A. Kaiser, "A reconfigurable IF to DC sub-sampling receiver architecture with embedded channel filtering for 60 GHz applications," *Circuits and Systems I: Regular Papers, IEEE Transactions on*, vol. 60, no. 5, pp. 1220–1231, May 2013.

[7] "IEEE standard - amendment 3: Enhancements for very high throughput in the 60 GHz band," *IEEE Std 802.11ad-2012 (Amendment to IEEE Std 802.11-2012)*, pp. 1–628, Dec 2012.

[8] R. Kimura *et al.*, "Golay sequence aided channel estimation for millimeter-wave WPAN systems," in *PIMRC 2008*. IEEE, 2008, pp. 1–5.

[9] J. G. Proakis and D. G. Manolakis, *Digital Signal Processing: Principles, Algorithms, and Applications, Fourth Ed.* Pearson Education, 2007.